Effect of the thermodynamic factor on the intrinsic and tracer diffusivities in binary mixtures

M. Sampayo Puelles ● and M. Hoyuelos ●[*]

Instituto de Investigaciones Físicas de Mar del Plata (IFIMAR – CONICET), Departamento de Física, Facultad de Ciencias Exactas y Naturales, Universidad Nacional de Mar del Plata, Deán Funes 3350, 7600 Mar del Plata, Argentina

One of the Darken equations gives a relationship between the intrinsic and the tracer diffusion coefficients, D_A and D_A^*, of species A in a solid binary mixture. In its original formulation, the equation reads $D_A = D_A^* \Gamma$, with Γ the thermodynamic factor. The question addressed in this paper is how D_A and D_A^* depend separately on Γ. Using a recent result for transition probabilities in terms of the excess chemical potential [M. Di Muro and M. Hoyuelos, Phys. Rev. E **104**, 044104 (2021)], it is shown that the intrinsic diffusivity does not depend on Γ. This approach simplifies a previous theoretical analysis that reaches the same result. Experimental results of diffusion in Ni-Pd and Fe-Pd alloys [M. J. H. van Dal *et al.*, Acta Mater. **48**, 385 (2000)] are used to check the theory. Numerical simulations of Ni-Pd were performed to show that the migration energy is the main factor responsible for the increase in diffusivity at intermediate concentrations.

I. INTRODUCTION

In 1948, Darken [1] obtained two equations to describe substitutional diffusion in solid binary mixtures, governed primarily by the presence of vacancies. Let us consider a binary mixture composed by species A and B that have molar concentrations c_A and c_B. The Darken equations represented a major advancement in the theoretical understanding of diffusion processes by establishing a connection between diffusivity and the thermodynamic factor, defined as $\Gamma = \beta \frac{\partial \mu_A}{\partial \log c_A}$, where $\beta = (k_B T)^{-1}$, and μ_A is the chemical potential (per particle) of species A. In terms of the excess chemical potential, the thermodynamic factor is $\Gamma = 1 + \beta \frac{\partial \mu_{\text{ex}}^A}{\partial \log c_A}$. It can be shown, through the Gibbs-Duhem relationship, that the thermodynamic factor is the same for both species.

The diffusion current (moles per unit area and time) for species A with respect to the crystalline lattice, along the x axis, is given by

$$j_A = -D_A \frac{\partial c_A}{\partial x}, \qquad (1)$$

where D_A is the intrinsic diffusion coefficient for species A, different, in general, from D_B; this difference gives rise to a volume flux through a plane of the lattice perpendicular to the current direction. In the laboratory reference frame, where volume flux is zero, A and B have the same diffusion coefficient, $\tilde{D}$, known as the interdiffusion coefficient and given by

$$\tilde{D} = v_B c_B D_A + v_A c_A D_B, \qquad (2)$$

where v_A and v_B are the partial molar volumes; see, for example, [2–4].

On the other hand, the diffusivity of a tagged particle of species A in the mixture is given by the tracer diffusion coefficient D_A^*, connected with the mobility, B_A, through the Einstein relation, $D_A^* = B_A RT$, where R is the ideal gas constant. Darken showed that D_A and D_A^* are related through the thermodynamic factor. More specifically,

$$D_A = D_A^* \frac{v_m}{v_B} \Gamma, \qquad (3)$$

where $v_m = N_A v_A + N_B v_B$ is the total molar volume, with N_A and N_B the mole fractions. Originally, Darken considered species with similar molar volumes such that $v_m \simeq v_A \simeq v_B$, and $D_A \simeq D_A^* \Gamma$. Combining Eqs. (2) and (3), the interdiffusion coefficient can be written as

$$\tilde{D} = (N_A D_B^* + N_B D_A^*) \Gamma. \qquad (4)$$

Equations (3) and (4) are known as Darken equations.

Information about how D_A and D_A^* separately depend on the thermodynamic factor was obtained in Ref. [5]. It was shown that the tracer diffusivity, D_A^*, behaves as $1/\Gamma$ and that the intrinsic diffusivity, D_A, does not depend on Γ. In this paper, we present an alternative and simpler derivation of the same results using an expression for transition rates in terms of the excess chemical potential that was recently derived in [6].

The paper is organized as follows. The form of transition rates is introduced in Sec. II. In Sec. III, it is demonstrated that the intrinsic diffusion coefficient does not depend on the thermodynamic factor. Numerical evaluation of the Debye frequency for the Ni-Pd alloy are also included in Sec. III in order to justify a linear approximation in its concentration dependence. Verification of the theoretical results using experimental data of the intrinsic diffusivity in solid mixtures of Ni-Pd and Fe-Pd, taken from Ref. [7], is presented in Sec. IV. The question of whether vacancy or migration energy is responsible of the observed increase in diffusivity at

---

*hoyuelos@mdp.edu.ar

024123-1

intermediate concentrations is addressed in Sec. V. Conclusions are presented in Sec. VI.

II. TRANSITION RATES

When vacancies and atoms of species A and B occupy sites of the same lattice we have a substitutional alloy. Movement of atoms through vacancies is the dominant diffusion mechanism in substitutional alloys. This is a frequent situation when atoms are of similar size. An atom has to overcome a migration energy in order to abandon its position in the lattice and, simultaneously, a vacancy should be present in the destination site. Then, the jump rate of an atom is characterized by two energies: the migration energy (of species A), G_M^A, and the vacancy formation energy, G_V. The combination of both is the activation energy: $G_A = G_M^A + G_V$ for species A. The jump rate for an atom of species A is

$$W_A = \omega_A e^{-\beta G_A}, \tag{5}$$

where ω_A is the jump attempt frequency of the order of the Debye frequency (see, for example, (Sec. 5.3.5 of [3])).

Equation (5) is based on a picture at the microscopic level since jumps between neighboring lattice sites are taken into account. Interactions at a thermodynamic level, represented by the excess chemical potential, are not explicitly represented in (5).

The thermodynamic aspects of transition rates and diffusivity are analyzed in Ref. [6]. A coarse grained picture is adopted in which microscopic details are lost. The system is divided into cells; each cell of size a has volume $V = a^3$ and contains many lattice sites. Two neighboring cells, labeled one and two, contain n_1 and n_2 atoms of species A, respectively. It can be demonstrated that the transition rate per particle between the two cells depends on the excess chemical potential in the following way [6]:

$$W_{n_1,n_2}^A = \nu_A \frac{e^{\beta \mu_{\text{ex},n_1}^A/2}}{\Gamma_{n_1}^{1/2}} \frac{e^{-\beta \mu_{\text{ex},n_2}^A/2}}{\Gamma_{n_2}^{1/2}}, \tag{6}$$

where the excess chemical potential and the thermodynamic factor with subindex n_i are evaluated at particle concentration n_i/V, and ν_A is a jump frequency, independent of the excess chemical potential; ν_A contains information of the substratum, such as the number of vacancies, that is not included in this coarse grained picture. The order of subindices in W_{n_1,n_2}^A indicates the jump direction from cell one to cell two. The derivation of (6) is based on statistical mechanics concepts, such as the detailed balance relationship and the Widom insertion formula; an outline is presented in the Appendix.

Equations (5) and (6) contain information at different levels. The main difference between them is that (5) is based on a microscopic picture of jumps between neighboring lattice sites, while jumps between cells containing many lattice sites are considered in the derivation of (6). This last approach allows an explicit representation of the transition rate dependence on the excess chemical potential. Both equations are used in the next section to obtain the intrinsic diffusion coefficient.

III. INTRINSIC DIFFUSION COEFFICIENT

The purpose of this section is to determine the dependence of the intrinsic diffusion coefficient, D_A, on the thermodynamic factor and on concentration. The transition rates (6) that contain the thermodynamic information can be used to calculate the particle current. Smooth spatial variations of the concentration are assumed. The average particle concentration is $\rho = \bar{n}/V$, and concentrations in each cell are $\rho_1 = n_1/V$ and $\rho_2 = n_2/V$, with $n_1 \simeq n_2 \simeq \bar{n}$. Let us assume that cells one and two are aligned along the x axis. The number of particles per unit time that jump between cells is $n_1 W_{n_1,n_2} - n_2 W_{n_2,n_1}$ and the area connecting cells is a^2. Then, the particle current is

$$
\begin{aligned}
J_A &= \left(n_1 W_{n_1,n_2}^A - n_2 W_{n_2,n_1}^A\right)/a^2 \\
&= \frac{\nu_A}{a^2 \left(\Gamma_{n_1} \Gamma_{n_2}\right)^{1/2}} \left(n_1 e^{-\beta \Delta \mu_{\text{ex}}^A/2} - n_2 e^{\beta \Delta \mu_{\text{ex}}^A/2}\right) \\
&\simeq \frac{\nu_A}{a^2 \Gamma}\left[n_1 - n_2 - \beta(n_1 + n_2)\Delta \mu_{\text{ex}}^A/2\right] \\
&\simeq -\frac{\nu_A}{a^2 \Gamma}\Delta n \underbrace{\left[1 + \beta \bar{n} \frac{\Delta \mu_{\text{ex}}^A}{\Delta n}\right]}_{\Gamma} = -\frac{\nu_A}{a^2}\Delta n \\
&= -\nu_A a^2 \frac{\Delta \rho}{a}, \tag{7}
\end{aligned}
$$

where $\Delta n = n_2 - n_1$ and $\Delta \mu_{\text{ex}}^A = \mu_{\text{ex},n_2}^A - \mu_{\text{ex},n_1}^A$. The particle current is proportional to the concentration gradient, $\Delta \rho/a$, that is, the first Fick's law, and the proportionality constant is the intrinsic diffusion coefficient:

$$D_A = \nu_A a^2. \tag{8}$$

The resulting coefficient is independent of the thermodynamic factor, or the excess chemical potential. This information is used below to support a simple approximation for the intrinsic diffusivity. The tracer diffusivity can also be obtained from transition rates in a mean field approximation (see Sec. II.C in [6]); in this case, the average jump rate in equilibrium is obtained by replacing n_1 and n_2 by the average $\bar{n}$ in Eq. (6) where the result is $W^A = \nu_A/\Gamma$. Using the continuous limit of a random walk with this transition rate, the tracer diffusivity is $D_A^* = W^A a^2 = \nu_A a^2/\Gamma = D_A/\Gamma$; that is, the Darken equation for species with approximately equal molar volumes. This result demonstrates the consistency of the present approach with the Darken equation.

From Eq. (5) we have

$$D_A \propto e^{-\beta G_A + \ln \omega}, \tag{9}$$

where ω is the Debye frequency, a function of the mole fraction N_A. The proportionality can be written in terms of the diffusivity, the activation energy and the Debye frequency in the limit of small concentration, D_{A0}, G_{A0}, and ω_0:

$$D_A = D_{A0} e^{-\beta(G_A - G_{A0}) + \ln(\omega/\omega_0)}. \tag{10}$$

(In the limit of small concentration of species A, interactions between A atoms can be neglected and we have that $D_A = D_A^* = D_{A0}$.)

Then, knowing that D_A does not depend on the excess chemical potential reduces the problem of determining the
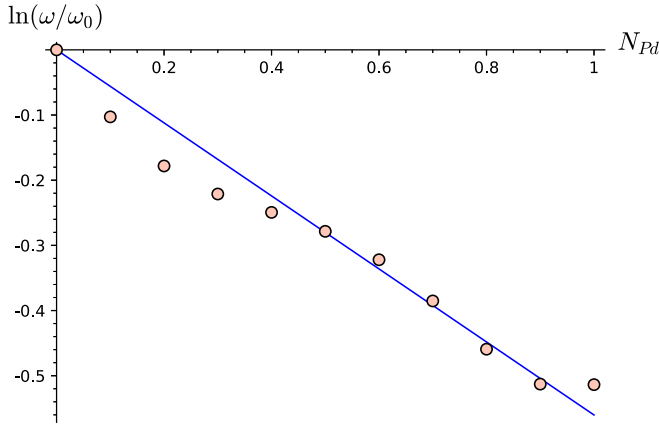
FIG. 1. Numerical results of the logarithm of the relative Debye frequency ω/ω_0 against Pd mole fraction, N_{Pd}, in a solid mixture Ni-Pd at zero temperature. The linear fit captures the approximately linear behavior. See Sec. III A for the simulation details.

concentration dependence of the intrinsic diffusivity to obtaining the concentration dependence of the activation energy G_A and the Debye frequency ω.

Molecular dynamics simulations were performed to obtain the Debye frequency for different mole fractions in a solid binary mixture of Ni-Pd at zero temperature; see Sec. III A for the methodology. The results are shown in Fig. 1; $\ln(\omega/\omega_0)$ has an approximately linear behavior against mole fraction. Some variation of the Debye frequency with temperature is expected; however, it is assumed that the linear behavior is preserved for different temperatures, so that

$$\ln(\omega/\omega_0) \simeq cN_A, \tag{11}$$

where c is a constant.

The two extreme values of the activation energy are G_{A0}, for $N_A = 0$, and G_{A1}, for $N_A = 1$. A simple expression for G_A based on Vegard's law is proposed. The activation energy is approximated by

$$G_A = N_A G_{A1} + N_B G_{A0} - \varepsilon_A N_A N_B, \tag{12}$$

where the first two terms correspond to the Vegard's law, a linear approximation between the two extreme values of G_A, and the last term is a possible deviation including the next nonlinear term in the molar fraction.

Replacing (11) and (12) in (10), and knowing that the value of the intrinsic diffusivity for the pure system is $D_{A1} = D_{A0}e^{-\beta(G_{A1}-G_{A0})+c}$, we have

$$D_A = D_{A0}^{N_B} D_{A1}^{N_A} e^{\beta\varepsilon_A N_A N_B}. \tag{13}$$

Using the Darken equation (3) combined with (10), the tracer diffusivity is

$$D_A^* = \frac{v_B}{v_m} \frac{1}{\Gamma} D_{A0} e^{-\beta(G_A-G_{A0})+\ln(\omega/\omega_0)}. \tag{14}$$

We obtained that D_A^* behaves as $1/\Gamma$. A concentration of vacancies in thermal equilibrium is assumed in the derivation of the Darken equation. This is an approximation that works in many cases, but it is not always valid. Vacancies are created and annihilated at opposite sites of the interdiffusion zone due to the volume flux (Kirkendall effect) that was mentioned

in the introduction. The Darken-Manning equations that consider the effect of vacancy-wind factors include necessary corrections; see, for example, (Sec. 10.4 of [2]). In order to avoid these difficulties, the comparison with experimental results presented in Sec. IV is restricted to the intrinsic diffusion coefficient.

The Darken equation has also been applied to surface diffusion; in general, the so-called correlation factor, f, has to be included to take into account memory effects. The tracer and collective diffusivities in the literature on surface diffusion [8–10] are usually written as

$$D^* = a^2 W f, \tag{15}$$

$$D = a^2 W \Gamma, \tag{16}$$

where the average jump rate W is a function of the coverage Θ. For example, for the Langmuir gas (hard core interaction), it is known that $W \propto 1 - \Theta$ and $\Gamma = 1/(1 - \Theta)$ (Sec. 2.6.2.3 of [9]); therefore, the dependence on Γ is canceled. The result we obtained can be thought of as a generalization since we demonstrate that the dependence on Γ for the collective (or intrinsic) diffusivity is canceled for any interaction.

This conclusion is consistent with other approaches. For example, a variational method [11,12] was proposed to calculate the collective diffusion of adsorbates on different surfaces taking into account microscopic details such as geometric aspects of the energy landscape, but the method does not use the thermodynamic information provided by Γ or the excess chemical potential.

A. Method to calculate the Debye frequency

The Debye frequency is given by

$$\omega = b \frac{v_s}{\alpha}, \tag{17}$$

where v_s is the sound speed, α is the lattice spacing, and b is a proportionality constant, equal to $(6\pi^2)^{1/3}$ for a cubic crystal [13]. The sound in a solid has longitudinal and transverse modes, each one with speeds given by

$$v_L = \sqrt{\frac{K + 4G/3}{\rho}}, \tag{18}$$

$$v_T = \sqrt{\frac{G}{\rho}}, \tag{19}$$

where K is the bulk modulus, G is the shear modulus, and ρ is the density [14]. Following Ref. [15], we use the average sound speed given by

$$v_s = 3/(2/v_T + 1/v_L). \tag{20}$$

The elastic constants, K and G, were calculated using LAMMPS software [16]. A box of $6 \times 6 \times 6$ unit cells of the Ni-Pd fcc lattice, with periodic boundary conditions, was considered. The box is deformed in different directions and the elastic constants are obtained from the change in the stress tensor. The procedure was repeated for different values of the mole fraction N_{Pd} from zero to one, using an average lattice spacing α that varies linearly from 3.521 (pure Ni) to 3.889 (pure Pd); the approximately linear behavior of α
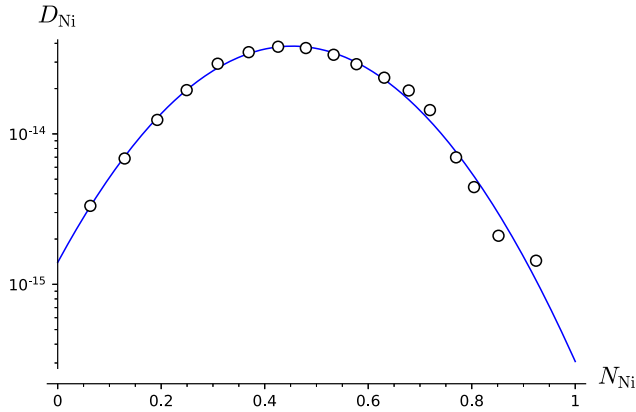
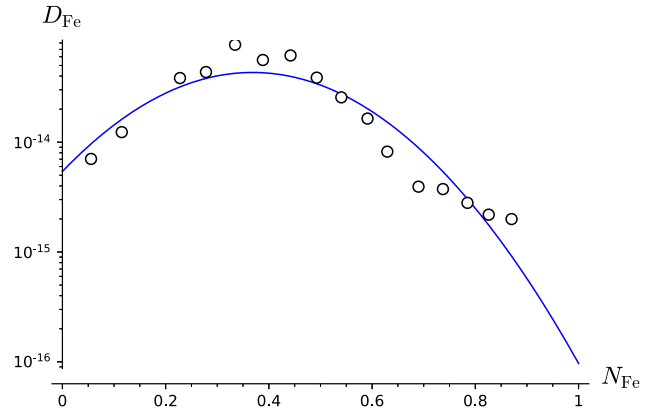(a) Intrinsic diffusivity for Ni in a Ni-Pd mixture.
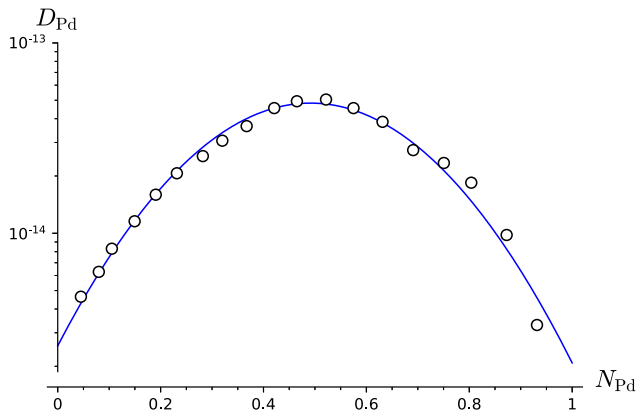
(b) Intrinsic diffusivity for Pd in a Ni-Pd mixture.

FIG. 2. Intrinsic diffusivities, D_{Ni} (a) and D_{Pd} (b) (units: m^2/s), in the Ni-Pd mixture against mole fraction. Circles correspond to experimental data of Ref. [7] and the curves correspond to Eq. (13) (see Table I for the parameters used).

(a) Intrinsic diffusivity for Fe in a Fe-Pd mixture.

(b) Intrinsic diffusivity for Pd in a Fe-Pd mixture.

FIG. 3. Intrinsic diffusivities, D_{Fe} (a) and D_{Pd} (b) (units: m^2/s), in the Fe-Pd mixture against mole fraction. Circles correspond to experimental data of Ref. [7] and the curves correspond to Eq. (13) (see Table I for the parameters used).
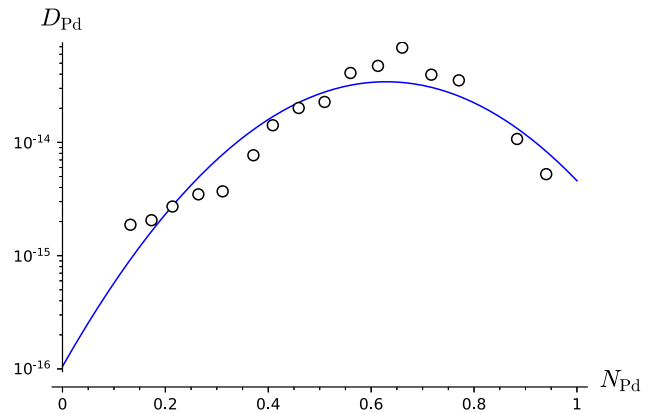
in Ni-Pd alloys was reported in [17]. The resulting value of ω was averaged over ten samples for each value of the mole fraction. The interaction potential in the Ni-Pd alloy was taken from the Interatomic Potentials Repository [18]; it is an angular-dependent potential of the Ni-Pd system, obtained by fitting the experimental data and first-principles calculations, reported in Ref. [19].

IV. COMPARISON WITH EXPERIMENTS

Equation (13) for the intrinsic diffusivity was compared with experimental results in Ref. [5] using data for the following mixtures: Au-Ni (at 900 °C) [20], Ag-Au (at 894 °C) [21], and Fe-Pd (at 1150 °C) [22]. Here we extend the experimental data set, including Ni-Pd (at 1100 °C) and Fe-Pd (at 1100 °C) [7], to further test the validity of the equation. The data used here for the mixture Fe-Pd, taken from Ref. [7], were obtained using an experimental technique (diffusion couple technique including incremental and "multi-foil" couples) that allows a direct measurement of intrinsic diffusivity; instead, in Ref. [22] the tracer diffusivity is measured and the intrinsic diffusivity is indirectly obtained from these measurements.

Figures 2 and 3 show the intrinsic diffusivities for Ni-Pd and Fe-Pd mixtures, respectively, against the corresponding mole fractions. The curves correspond to Eq. (13) with adjusted values of D_0, D_1, and $\beta\varepsilon$ (sub-index A is omitted for simplicity). It can be seen that the equation satisfactorily represents the data, specially for the Ni-Pd mixture. Table I contains the values used for D_0, D_1, and $\beta\varepsilon$ in each case.

In the limit $N_A \to 1$, D_{A1} is the self-diffusion coefficient of species A; it can be obtained from Table 13.1 in Ref. [23]; the reference values for Ni, Pd, and Fe at 1100 °C are $D_{Ni,1} = 0.261$, $D_{Pd,1} = 0.153$, and $D_{Fe,1} = 0.06$, with units 10^{-14} m^2/s. The differences with the values of Table I can

TABLE I. Adjusted parameters of Eq. (13) for each metal in their respective alloy. Units for D_0 and D_1 are 10^{-14} m^2/s.

	D_0	D_1	$\beta\varepsilon$
Ni	0.14	0.031	16.1
Pd	0.26	0.21	12.2
Fe	0.54	0.01	15.3
Pd	0.01	0.46	14.6

be understood as a consequence of the simple form assumed for the activation energy (12). Despite these discrepancies, the approximation for G_A is still able to provide a good description of the intrinsic diffusivity in the whole range of the mole fraction.

V. VACANCY VERSUS MIGRATION ENERGY

In all the mixtures analyzed, here and in Ref. [5], positive values of the nonlinear term parameter, ε_A, were obtained. This means that the diffusivity is larger than the value predicted by Vegard's law for intermediate concentrations. The mixture enhances the diffusivity. The activation energy is the sum of the migration and the vacancy formation energies, $G_A = G_M^A + G_V$. It is interesting to establish whether the migration energy or the vacancy formation energy is the main thing responsible for the increase in diffusivity at intermediate concentrations. A possible interpretation of the results is that, for intermediate concentrations, the mixture of atoms with different sizes introduces a disorder in the lattice that favors the vacancy formation. But this is not actually the case. Numerical simulations show that the vacancy formation energy does not decrease in the mixture. On the contrary, in Ref. [24] it was shown that an illustrative generic alloy system with ordering tendencies has a vacancy formation energy that increases at intermediate concentrations, meaning that the mean number of vacancies is smaller than the value predicted by Vegard's law; see Fig. 16 in [24]. A qualitatively similar result was obtained in [25] for a high entropy alloy using grand-canonical lattice Monte Carlo simulations; in this case the vacancy formation energy is slightly above Vegard's law. These results indicate that the observed increase in diffusivity with respect to Vegard's law at intermediate concentrations is more likely a consequence of a decrease in migration energy than in vacancy formation energy. This supposition was checked with numerical simulations of the mixture Ni-Pd in which the migration energy was calculated; see Sec. V A for the methodology. The results obtained are shown in Fig. 4; they present a decrease of the migration energy for intermediate concentrations.

A. Method to calculate migration energy

The migration energy was calculated using LAMMPS software [16] and the nudged elastic band method (NEB). The NEB allows to find the height of an energy barrier associated with a transition state. In this case we use it for the transition of an atom toward a vacancy.

As in Sec. III A, a box of $6 \times 6 \times 6$ unit cells of Ni-Pd fcc lattice with periodic boundary conditions was considered, and the interaction potential reported in Ref. [19] was used; a linear behavior for the lattice spacing α as a function of mole fraction was also assumed [17]. A vacancy is created in the lattice, and the species (Ni or Pd) of a first neighbor is set as the initial configuration; this atom is the one that will perform the hop. The final configuration corresponds to the vacancy at the site of the jumping atom and the atom at the site where the vacancy was initially found.

For the hop of a Ni atom we considered 2000 different configurations of atoms in the mole fraction N_{Pd} range from
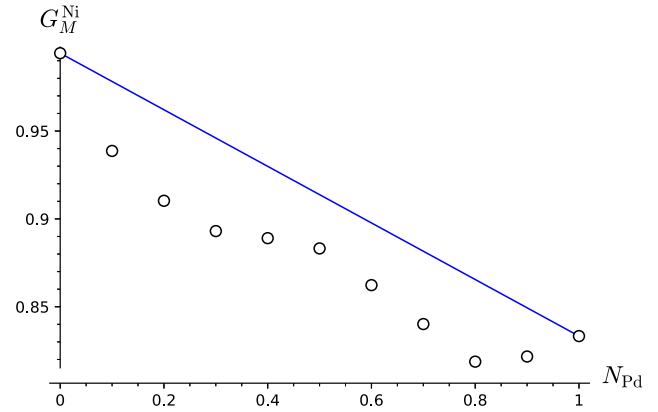
(a) Migration energy of Ni in a Ni-Pd mixture.
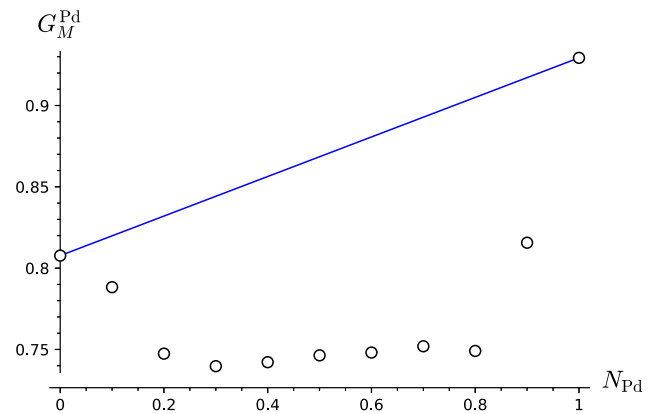
(b) Migration energy of Pd in a Ni-Pd mixture.

FIG. 4. Numerical results of migration energy of Ni and Pd, G_M^{Ni} (a) and G_M^{Pd} (b) (units: eV), in a Ni-Pd solid mixture, against mole fraction, using the angle-dependent potential of Ref. [19]. The line corresponds to Vegard's law. See Sec. V A for the simulation details.

0.1 to 0.9. Note that for N_{Pd} equal to zero or one it is not necessary to average different configurations, since all atoms are of the same type. For the case of Pd, 1000 realizations were enough.

We perform NEB calculations for six replicas, the first and last are the initial and the end point of the transition path. During the NEB calculation the set of replicas converge toward a minimum energy path of conformational states that transition over a barrier. The configuration of highest energy along the path corresponds to a saddle point, and the potential energies for the set of replicas represents the energy profile of the transition along the minimum energy path.

Migration energy is the energy of the barrier, which is the difference in energy between the saddle point and the first replica. Both the final and initial replicas have approximately the same energy.

VI. CONCLUSIONS

The Darken equation (3) gives a relationship between the intrinsic and the tracer diffusion coefficients, D_A and D_A^*, through the thermodynamic factor Γ. Nevertheless, it does not provide information about how D_A and D_A^* separately

depend on Γ. This problem was addressed in Ref. [5], where it was shown that the intrinsic diffusivity does not depend on Γ. Here, we arrive at the same result using a general expression for transition rates that contains information at the thermodynamic level, that is, the expression determines how transition rates depend on the excess chemical potential [6]. A more direct derivation is obtained in this way; one important simplification is that it is not necessary to apply the concept of "interpolation parameter" used in [5]. The procedure provides a deeper understanding of the problem of the dependence of diffusivity on the thermodynamic factor.

It is well known that vacancies play a fundamental role in substitutional diffusion. According to our result, the concentration dependence of the intrinsic diffusivity is completely determined by the Debye frequency and the form of the activation energy G_A, that includes the vacancy formation energy and the migration energy (as usual, experiments are more complicated than theoretical idealizations; some ingredients that are not taken into account, and that may be relevant, are, for example, the presence of impurities or the impurity vacancy binding energy; see [26]). Numerical simulations of the Ni-Pd alloy show that the Debye frequency behaves approximately linearly as a function of the mole fraction. A simple form for G_A against mole fraction is proposed using Vegard's law and including a quadratic term proportional to parameter ε. This approximation allows a theoretical description of the dependence of the intrinsic diffusivity on mole fraction, see Eq. (13). Experimental data of diffusion in Ni-Pd and Fe-Pd mixtures [7] are consistent with the theoretical results. Positive values of ε were obtained; this implies diffusion coefficient values that are larger than a linear interpolation between D_{A0} and D_{A1}, for mole fractions zero and one, respectively. Regarding the question of whether this increase in diffusivity with respect to Vegard's law is mainly a consequence of a decrease in the migration energy or the vacancy formation energy, numerical simulation of other authors suggest that vacancy formation energy actually increases at intermediate concentrations. Therefore, the diffusivity increase at intermediate concentrations should be a consequence of a decrease of migration energy. Such decrease of the migration energy was numerically observed in the solid mixture of Ni-Pd.

Equation (13) in logarithmic scale has the form of a parabola. A parabolic form for the intrinsic diffusion coefficient against concentration is assumed as a hypothesis in Refs. [27,28] where a method for calculating intrinsic diffusivities in multi component systems is proposed.

APPENDIX: DERIVATION OF TRANSITION RATES

A short version of the derivation of transition rates, Eq. (6), is presented in this Appendix (the full version can be found in [6]). The demonstration refers to a system of particles in contact with a reservoir at temperature T and chemical potential μ. The system is divided into cells; cell i contains n_i particles. Spatial and temporal variations are smooth and local thermal equilibrium holds. Interaction energy at cell walls is neglected with respect to the bulk.

We analyze transitions between cells one and two, with n_1 and n_2 particles. The initial state is $A = \{n_1, n_2\}$, and, after a jump from one to two, the final state is $B = \{n_1 - 1, n_2 + 1\}$. Transition rate from A to B is $W_{A,B}$. Local equilibrium is a sufficient condition for detailed balance:

$$P_A W_{A,B} = P_B W_{B,A}, \tag{A1}$$

where P_A and P_B are the probabilities of states A and B.

The canonical partition function of a cell is $\mathcal{Z}_n$; it depends on number of particles n, temperature T, and Ω, a measure of the cell's volume given by the number of microscopic states for one particle. In the absence of interactions, the canonical partition function is equal to the total number of microstates: $\mathcal{Z}_{0,n} = \Omega^n / n!$ (for a continuous system, $\Omega = V/\lambda^3$, where λ is the thermal de Broglie wavelength and V is the cell's volume).

The grand partition function for a cell is given by

$$\mathcal{Q} = \sum_{n=0}^{\infty} e^{\beta \mu n} \mathcal{Z}_n. \tag{A2}$$

The probability of having n particles is $P_n = e^{\beta \mu n} \mathcal{Z}_n / \mathcal{Q}$. The probabilities for states A and B are $P_A = P_{n_1} P_{n_2}$ and $P_B = P_{n_1-1} P_{n_2+1}$. Then, Eq. (A1) implies

$$\mathcal{Z}_{n_1} \mathcal{Z}_{n_2} W_{A,B} = \mathcal{Z}_{n_1-1} \mathcal{Z}_{n_2+1} W_{B,A}. \tag{A3}$$

We define the configuration energy, ϕ_n, as

$$e^{-\beta \phi_n} = \frac{\mathcal{Z}_n}{\mathcal{Z}_{0,n}}, \tag{A4}$$

so that, in the thermodynamic limit, ϕ is equal to the excess free energy F_{ex} (quantities without subindex n are evaluated at the mean value $\bar{n}$). Using the definition of ϕ_n, Eq. (A3) leads to

$$\frac{W_{A,B}}{W_{B,A}} = \frac{e^{-\beta(\phi_{n_2+1}-\phi_{n_2})}}{e^{-\beta(\phi_{n_1}-\phi_{n_1-1})}} \frac{n_1}{n_2 + 1}. \tag{A5}$$

Since all particles are equivalent, the jump rate for one particle in cell one is $W_{A,B}/n_1$. Defining $W_{n_1,n_2} = W_{A,B}/n_1$ and $W_{n_2+1,n_1-1} = W_{B,A}/(n_2+1)$, Eq. (A5) becomes

$$W_{n_1,n_2} \, e^{-\beta(\phi_{n_1}-\phi_{n_1-1})} = W_{n_2+1,n_1-1} \, e^{-\beta(\phi_{n_2+1}-\phi_{n_2})}. \tag{A6}$$

The order of subscripts in W_{n_i,n_j} indicates the jump direction.

The next step is to apply the Widom insertion formula ([29], see p. 30 of [30]):

$$e^{-\beta \mu_{\mathrm{ex}}} = \langle e^{-\beta \, \Delta \phi_n} \rangle, \tag{A7}$$

where $\Delta \phi_n = \phi_{n+1} - \phi_n$, and the angular brackets represent the average in the grand canonical ensemble. See Appendix A in Ref. [6] for a derivation of the Widom insertion formula in the grand canonical ensemble.

We need expressions for the differences $\phi_{n_1} - \phi_{n_1-1}$ and $\phi_{n_2+1} - \phi_{n_2}$ that appear in (A6). Using (A7), it can be shown that (see Appendix B in [6]),

$$\phi_{n_2+1} - \phi_{n_2} = \mu_{\mathrm{ex},n_2} + \varepsilon_{n_2} + \mathrm{h.t.}, \tag{A8}$$

$$\phi_{n_1} - \phi_{n_1-1} = \mu_{\mathrm{ex},n_1} + \varepsilon_{n_1} + \mathrm{h.t.}, \tag{A9}$$

where $\mu_{\text{ex},n_i} \sim O(\Omega^0)$ and $\varepsilon_{n_i} \sim O(1/\Omega)$. Higher order terms are represented by "h.t.". Equation (A6) becomes

$$W_{n_1,n_2}\, e^{-\beta(\mu_{\text{ex},n_1}+\varepsilon_{n_1}+\text{h.t.})} = W_{n_2+1,n_1-1}\, e^{-\beta(\mu_{\text{ex},n_2}+\varepsilon_{n_2}+\text{h.t.})}. \tag{A10}$$

As usual in thermodynamics, we consider that the configuration energy or the transition rates are continuous functions of the number of particles, so that $W_{n_2+1,n_1-1} = W_{n_2,n_1} + \partial_{n_2} W_{n_2,n_1} - \partial_{n_1} W_{n_2,n_1} + \text{h.t.}$, and, from Eq. (A10), we have

$$
\begin{aligned}
W_{n_1,n_2}\, e^{-\beta\mu_{\text{ex},n_1}} &\left(1 - \beta\varepsilon_{n_1} + \text{h.t.}\right) \\
&= \left(W_{n_2,n_1} + \partial_{n_2} W_{n_2,n_1} - \partial_{n_1} W_{n_2,n_1}\right. \\
&\quad \left. - \beta\varepsilon_{n_2} W_{n_2,n_1} + \text{h.t.}\right) e^{-\beta\mu_{\text{ex},n_2}}.
\end{aligned} \tag{A11}
$$

Since the particle number is an extensive quantity, the transition rate derivatives are of order $1/\Omega$.

We separate terms at orders Ω^0 and Ω^{-1} (higher order terms are not necessarily negligible):

$$\mathcal{O}(\Omega^0): \quad W_{n_1,n_2} e^{-\beta\mu_{\text{ex},n_1}} = W_{n_2,n_1} e^{-\beta\mu_{\text{ex},n_2}} \tag{A12}$$

$$
\begin{aligned}
\mathcal{O}(\Omega^{-1}): &-\beta\varepsilon_{n_1} W_{n_1,n_2} e^{-\beta\mu_{\text{ex},n_1}} \\
&= \left(\partial_{n_2} W_{n_2,n_1} - \partial_{n_1} W_{n_2,n_1} - \beta\varepsilon_{n_2} W_{n_2,n_1}\right) e^{-\beta\mu_{\text{ex},n_2}}.
\end{aligned} \tag{A13}
$$

It can be shown (see Appendix B in [6]) that

$$\varepsilon_{n_2} = -\frac{1}{2\beta}\frac{\Gamma'_{n_2}}{\Gamma_{n_2}} + \mu'_{\text{ex},n_2}/2, \tag{A14}$$

$$\varepsilon_{n_1} = -\frac{1}{2\beta}\frac{\Gamma'_{n_1}}{\Gamma_{n_1}} - \mu'_{\text{ex},n_1}/2, \tag{A15}$$

where primed quantities are derivatives in respect to the particle number. Combining (A12) and (A13) we get

$$
\begin{aligned}
\left(\partial_{n_2} - \partial_{n_1}\right)\ln W_{n_2,n_1} &= \beta\left(\varepsilon_{n_2} - \varepsilon_{n_1}\right) \\
&= -\frac{\Gamma'_{n_2}}{2\Gamma_{n_2}} + \frac{\beta}{2}\mu'_{\text{ex},n_2} + \frac{\Gamma'_{n_1}}{2\Gamma_{n_1}} + \frac{\beta}{2}\mu'_{\text{ex},n_1}.
\end{aligned} \tag{A16}
$$

The following ansatz is proposed:

$$W_{n_2,n_1} = \nu_{n_2,n_1}\frac{1}{\left(\Gamma_{n_2}\Gamma_{n_1}\right)^{1/2}}\frac{e^{\beta\mu_{\text{ex},n_2}/2}}{e^{\beta\mu_{\text{ex},n_1}/2}}. \tag{A17}$$

W_{n_1,n_2} is obtained by exchanging $n_1 \leftrightarrow n_2$. Replacing the ansatz in (A12) and (A16) we obtain the following conditions for ν_{n_2,n_1}:

$$\nu_{n_2,n_1} = \nu_{n_1,n_2}, \tag{A18}$$

$$\partial_{n_2}\ln\nu_{n_2,n_1} = \partial_{n_1}\ln\nu_{n_2,n_1}. \tag{A19}$$

The solution for ν_{n_2,n_1} is a function that depends on the sum $n_1 + n_2$, and can be written as $\nu_{n_2+n_1}$. Then, the transition rate is

$$W_{n_2,n_1} = \nu_{n_2+n_1}\frac{e^{-\beta\mu_{\text{ex},n_1}/2}}{\Gamma_{n_1}^{1/2}}\frac{e^{\beta\mu_{\text{ex},n_2}/2}}{\Gamma_{n_2}^{1/2}}, \tag{A20}$$

that is, Eq. (6) (with $n_1 \leftrightarrow n_2$). The jump frequency ν represents effects of the substratum that, in general, may depend on concentration (the average concentration in both cells); this kind of information depends on microscopic details, such as the energy barrier landscape, and cannot be inferred using the present coarse-grained approach.

[1] L. S. Darken, Diffusion, mobility and their interrelation through free energy in binary metallic systems, Trans. AIME **175**, 184 (1948).

[2] H. Mehrer, *Diffusion in Solids* (Springer, Berlin, 2007).

[3] A. Paul, T. Laurila, V. Vuorinen, and S. V. Divinski, *Thermodynamics, Diffusion and the Kirkendall Effect in Solids* (Springer, Heidelberg, 2014).

[4] P. Shewmon, *Diffusion in solids* (Springer, Cham, 2016).

[5] M. Di Pietro Martínez and M. Hoyuelos, Diffusion in binary mixtures: an analysis of the dependence on the thermodynamic factor, Phys. Rev. E **100**, 022112 (2019).

[6] M. Di Muro and M. Hoyuelos, Application of the Widom insertion formula to transition rates in a lattice, Phys. Rev. E **104**, 044104 (2021).

[7] M. J. H van Dal, M. C. L. P. Pleumeekers, A. A. Kodentsov, and F. J. J. van Loo, Intrinsic diffusion and Kirkendall effect in Ni-Pd and Fe-Pd solid solutions, Acta Mater. **48**, 385 (2000).

[8] T. Ala-Nissila, R. Ferrando, and S. C. Ying, Collective and single particle diffusion on surfaces, Adv. Phys. **51**, 949 (2002).

[9] R. Gomer, Diffusion of adsorbates on metal surfaces, Rep. Prog. Phys. **53**, 917 (1990).

[10] D. A. Reed and G. Ehrlich, Surface diffusion, atomic jump rates and thermodynamics, Surf. Sci. **102**, 588 (1981).

[11] M. A. Załuska-Kotur, and Z. W. Gortel, Ritz variational principle for collective diffusion in an adsorbate on a non-homogeneous substrate, Phys. Rev. B **76**, 245401 (2007).

[12] M. Mińkowski and M. A. Załuska-Kotur, Collective diffusion of dense adsorbate at surfaces of arbitrary geometry, J. Stat. Mech. (2018) 053208.

[13] C. Kittel, *Introduction to Solid State Physics*, 8th ed. (John Wiley & Sons, 2005).

[14] L. E. Kinsler, A. R. Frey, A. B. Coppens, and J. V. Sanders, *Fundamentals of acoustics*, 4th ed. (John Wiley & Sons, 2000).

[15] M. G. Holland, Analysis of lattice thermal conductivity, Phys. Rev. **132**, 2461 (1963).

[16] S. Plimpton, Fast parallel algorithms for short-range molecular dynamics, J. Comput. Phys. **117**, 1 (1995), see http://lammps.sandia.gov.

[17] L. R. Bidwell, Unit-cell dimensions of Ni-Pd alloys at 25 and 900° C, Acta Cryst. **17**, 1473 (1964).

[18] Interatomic Potentials Repository, https://www.ctcms.nist.gov/potentials.

[19] Y. Xu, G. Wang, P. Qian, and Y. Su, Element segregation and thermal stability of Ni-Pd nanoparticles, J. Mater. Sci. **57**, 7384 (2022).

[20] J. E. Reynolds, B. L. Averbach, and M. Cohen, Self-diffusion and interdiffusion in gold-nickel alloys, Acta Metall. **5**, 29 (1957).

[21] H. W. Mead and C. E. Birchenall, Diffusion in gold and Au-Ag alloys, JOM **9**, 874 (1957).

[22] J. Fillon and D. Calais, Autodiffusion dans les alliages concentres fer-palladium, J. Phys. Chem. Solids **38**, 81 (1977).

[23] Y. Sohn, Diffusion in metals, in *Smithells Metals Reference Book*, 8th ed., edited by W. F. Gale and T. C. Totemeier (Elsevier, Oxford, 2004).

[24] X. Zhang and M. H. F. Sluiter, Ab initio prediction of vacancy properties in concentrated alloys: The case of fcc Cu-Ni, Phys. Rev. B **91**, 174107 (2015).

[25] Daniel Utt, Alexander Stukowski, and Karsten Albe, Thermodynamics of vacancies in concentrated solid solutions:

From dilute ni-alloys to the cantor system, arXiv:2104.02697 (2021).

[26] S. Santra, H. Dong, T. Laurila, and A. Paul, Role of different factors affecting interdiffusion in Cu(Ga) and Cu(Si) solid solutions, Proc. R. Soc. A **470**, 20130464 (2014).

[27] B. Wierzba and W. Skibiński, The generalization of the Boltzmann-Matano method, Physica A **392**, 4316 (2013).

[28] B. Wierzba and W. Skibiński, The intrinsic diffusivities in multi component systems, Physica A **440**, 100 (2015).

[29] B. Widom, Some topics in the theory of fluids, J. Chem. Phys. **39**, 2808 (1963).

[30] J.-P. Hansen and I. R. McDonald, *Theory of Simple Liquids: with Applications to Soft Matter* (Academic Press, Oxford, 2013).